MASTER COPY KEEP THIS COPY FOR REPRODUCTION PURPOSES

REPORT DOCUMENTATION PAGE

Form Approved
OMB No. 0704-0188

...is estimated to average 1 hour per response, including the time for reviewing instructions, searching existing data sources, ...ting and reviewing the collection of information. Send comments regarding this burden estimate or any other aspect of this ...cing this burden to Washington Headquarters Services, Directorate for Information Operations and Reports, 1215 Jefferson ...id to the Office of Management and Budget, Paperwork Reduction Project (0704-0188), Washington, DC 20503

AD-A244 389

2. REPORT DATE	3. REPORT TYPE AND DATES COVERED
6/20/91	Final Report 9/15/87 - 3/14/91

Theoretical and Experimental Investigation of Electron Beam Acceleration and Submillimeter Wave Generation in Cyclotron Resonant Cavities

5. FUNDING NUMBERS

DAAL03-87-K-0139

(2)

6. AUTHOR(S)

N.C. Luhmann, Jr., D.B. McDermott

DTIC ELECTE JAN 14 1992 S D D

7. PERFORMING ORGANIZATION NAME(S) AND ADDRESS(ES)

University of California, Los Angeles
405 Hilgard Avenue
Los Angeles, CA 90024

8. PERFORMING ORGANIZATION REPORT NUMBER

9. SPONSORING/MONITORING AGENCY NAME(S) AND ADDRESS(ES)

U. S. Army Research Office
P. O. Box 12211
Research Triangle Park, NC 27709-2211

10. SPONSORING/MONITORING AGENCY REPORT NUMBER

ARO 24861.5-PH

11. SUPPLEMENTARY NOTES

The view, opinions and/or findings contained in this report are those of the author(s) and should not be construed as an official Department of the Army position, policy, or decision, unless so designated by other documentation.

12a. DISTRIBUTION AVAILABILITY STATEMENT

Approved for public release; distribution unlimited.

12b. DISTRIBUTION CODE

13. ABSTRACT (Maximum 200 words)

Many millimeter wave generation interactions have been under development. A prebunched high harmonic gyrotron has extended the power level of our previous high harmonic gyrotrons. Also, the instabilities in gyro-TWT amplifiers are now understood and methods have been formulated to stabilize them (multi severs). This work has led to the design of a very high power (500 kW) harmonic gyro-TWT using a conventional MIG, which we plan to build in the next few years. We have also been active in the development of an extremely high power millimeter wave source, the CARM: 1) we have designed and simulated a 300 MW, 17 GHz device for the next generation high gradient rf linac; 2) we actively participated in LLNL's 250 GHz CARM project; and 3) we are continuing to fabricate at UCLA a 400 kV, 10 MW proof of principle CARM, which will use Bragg reflectors for its requisite frequency selective cavity. We have advanced the state-of-the-art of Bragg reflectors by testing high mode purity Bragg reflectors. In addition, we have designed and are well into the construction of a very high power, wideband continuous tunability gyro-BWO and a very efficient gyro-klystron amplifier.

14. SUBJECT TERMS

Gyrotron, TE_{11} rf accelerator, TE_{nl} interaction cavity, Gyro-TWT, Gyro-BWO, sever, Bragg reflector, Hamming-Window taper, CARM, magnetic taper, autoresonance, MIG, gyro-klystron

15. NUMBER OF PAGES

16. PRICE CODE

17. SECURITY CLASSIFICATION OF REPORT	18. SECURITY CLASSIFICATION OF THIS PAGE	19. SECURITY CLASSIFICATION OF ABSTRACT	20. LIMITATION OF ABSTRACT
UNCLASSIFIED	UNCLASSIFIED	UNCLASSIFIED	UL

BRIEF LIST OF RESEARCH FINDINGS

1. Prebunched Harmonic Gyrotron

Our high harmonic gyrotron program has evolved into wave generation from prebunched electron beams. A new scheme for harmonic wave generation using a prebunched electron beam has been demonstrated. Due to the prebunched nature of the helical electron beam generated by the gyroresonant TE_{11} RF accelerator, all electrons can be injected into the gyrotron at the optimum phase. Since the helix rotates at the accelerator's RF frequency, ω_{acc}, each electron will see the same phase when entering the TE_{n1} interaction cavity with frequency, ω, if $\omega = n\omega_{acc}$. The prebunched electron beam has been used to further increase the efficiency of our axis–encircling high harmonic gyrotron. The proof–of–principle experiment was performed at the third harmonic with a TE_{312} mode at 27.7 GHz. The conversion power of 6.7 kW was significantly greater than that of the non–prebunched experiment. Also, mode competition was effectively suppressed. As expected, the output power is proportional to the square of the electron beam current and the start of oscillation current is essentially zero. A linear theory, derived by taking into account the spread of the guiding center and the spread of the axial velocity, gives good agreement with the experimental result, as shown in Fig. 1. A manuscript describing this work has been published in the special issue on High-Power Microwave Generation of the IEEE Transactions on Plasma Science (Vol. 18, p. 343-349 (1990)).

2. Gyro-TWT Amplifier

A gyro-TWT amplifier is a device with great promise - high power and efficiency as for the gyrotron and very high gain - but with a history of unsatisfactory performance. One reason for the poor behavior is that this device oscillates too easily. The initial goal of our gyro-TWT program is to operate a stable gyro-TWT amplifier.

In order to obtain a stable gyro-TWT amplifier, it is necessary to first suppress oscillation in the device. The graduate student, Mr. C.S. Kou, has therefore focussed his attention on gyro-TWT stability. He has developed an analytical theory based on Laplace transforms which can account for the two known sources of oscillation, both the absolute instability and the gyro-BWO. A comparison between his linear theory and the nonlinear self-consistent simulation code he also wrote is shown in Fig. 2. The agreement is seen to be excellent in the linear region where they are both applicable. His theory verifies the well known fact that the absolute instability at the cutoff frequency can be turned off by reducing the beam current below the threshold value, I_s. In addition, his theory has allowed us to study an important new effect. The gyro-BWO can be suppressed by keeping the interaction length less than the starting length for oscillation, L_s. The dependence of this critical length on beam current is shown in Fig. 3 for the parameters of our gyro-TWT experiment. Thus, a stable gyro-TWT should operate with a beam current less than I_s and consist of several interaction sections with with a length less than L_s.

Another important phenomenon has been studied with this new theory. A second harmonic gyro-TWT with an axis-encircling beam can deliver much higher power than a fundamental gyro-TWT. This is because higher beam current is allowed since I_s is much higher

92-00690

due to the weaker interaction. Yet, the predicted conversion efficiency is nearly the same as in the fundamental device. In a fundamental TE_{11} gyro-TWT, the major gyro-BWO threat is from the TE_{21} mode at the second harmonic as shown in the uncoupled dispersion diagram shown in Fig. 4(a), whereas the major BWO threat in a second harmonic TE_{21} gyro-TWT is at the third harmonic in the TE_{31} mode, as seen in Fig. 4(b). However, it is much easier to suppress the third harmonic BWO in the second harmonic TWT than the second harmonic BWO in the fundamental TWT. A stable 830 kW second harmonic gyro-TWT can be achieved with only two sections, while a stable fundamental gyro-TWT requires at least three sections and could deliver a power of at most 100 kW. Table 1 lists the parameters for optimized first and second harmonic gyro-TWTs. The predicted performance of the second harmonic device is considerably superior. Since it has the negative feature that it requires an axis-encircling electron beam, we have also investigated whether the positive features of a second harmonic gyro-TWT can be attained while using a conventional MIG and found that they can! A 100 kV, 25 A MIG gun with 5% axial velocity spread can generate 500 kW at the second harmonic in the TE_{21} mode with over 30 dB of gain.

3. Bragg Reflectors

We are also developing Bragg reflectors for selective feedback in overmoded oscillators. Though gyro-TWT and Cyclotron Autoresonance Maser (CARM) oscillators are of immediate interest, a Bragg reflector is applicable to many convective growth interactions. A cylindrical corrugated metal waveguide will scatter a forward wave with wavevector, $k_{||}$, into a backward wave if the corrugation period, ℓ, satisfies the Bragg condition, $k_{||} = \pi/\ell$. A Bragg resonator is comprised of two sections of corrugated waveguide surrounding a smooth cavity section. Since it is merely a perturbation of the wall, a Bragg reflector is conducive to beam transport.

We fabricated and tested Bragg reflectors with rectangular corrugation and with sinusoidal corrugation. Both worked well. We found that an undesirable complication of Bragg reflectors is that they can covert a wave into another mode. In our reflectors, which were designed for the TE_{11} mode, this mode would readily convert to the TM_{11} mode if the corrugation amplitude was too large. Fortunately, a solution was found after we entered into a collaboration with Dr. M. Thumm of Stuttgart University.

Using design rules from filter theory, Dr. Thumm designed a tapered corrugation reflector to reduce mode conversion and give a narrower and smoother frequency response. The Hamming-Window amplitude distribution is given by

$$h(x) = A * (0.54 - 0.46\,cos(2\pi x/L))$$

where h(x) is the amplitude of the corrugation at position x (distance is measured from the beginning of the reflector of length L) and A is the peak amplitude of the corrugation. Two units have been fabricated with the parameters listed in Table 2 and measured with an automated network analyzer. The results from Thumm's scattering matrix code of a Hamming-Window Bragg with a reflectivity of 99.4% are compared in Fig. 5 with the measurement data. The taper allows a much larger corrugation amplitude to be used and therefore can yield a reflection very close to unity. Figure 6 compares the measurements of a Hamming-Window Bragg with a reflectivity of 96% with the prediction from the scattering

92 1 8 080

matrix code. The agreement is again seen to be excellent. This Bragg with the lower reflectivity will be used as the output reflector of our 400 kV CARM oscillator experiment and the higher reflectivity Bragg will be used as the upstream reflector to shield the electron gun.

4. High Power CARM

We have designed a 150 MW, 17 GHz CARM (Cyclotron Autoresonance Maser) amplifier which can satisfy DOD's need for super power microwave sources as well as DOE's driver requirements for future high gradient rf linacs. CARMs are similar to gyro-TWTs and are of interest because of their high efficiency, which is due to their autoresonant feature that the electrons do not fall out of gyroresonance with a copropagating wave with $\omega = ck_z$. The design is shown in Table 3 and will yield 40% efficiency for a readily achievable axial velocity spread of 4% if the magnetic field is properly tapered. We have found the conditions for optimal linear magnetic taper. Figure 7 shows the effect of magnetic field taper on the enhancement of efficiency,where the axially applied magnetic field is down-tapered at a rate of 1.4%/cm, but started from different locations. Notice that tapering can substantially increase the efficiency and furthermore that the degree of enhancement depends on the starting position. Figure 8 shows the electron phase (ϕ) as a function of the axial position. One may determine where to start the magnetic taper by studying the electron phase plot of the untapered case shown in Fig. 8(a). Electrons begin to crossover at z = 100 cm for the particular case shown. This is where the taper should begin. In Fig. 8(b), the taper begins at z = 118 cm, just before saturation but well after the initial crossover. We can see that the magnetic filed taper enhances the efficiency by channeling more electrons in to the decelerating phase (from 0 to -π) and keeping them there longer. Figure 8(c) illustrates the phase plot of the case where the same magnetic field taper starts at z = 100 cm where the initial crossover occurs. This time the magnetic taper drags the whole bunch more deeply into the decelerating phase and, therefore, a higher efficiency than the other two cases is achieved.

We have nearly completed the construction of a moderate voltage (400 kV) CARM oscillator proof of principle experiment. The modulator has been built and tested, a 400 kV electron gun obtained (from SLAC), and the cavity has been fabricated and tested. Just as in a gyro-TWT, the gyro-BWO is also going to be a serious threat in our 400 kV CARM oscillator experiment. It will be necessary to keep the beam current less than the BWO's I_s for a given interaction length. To preferentially excite the high frequency mode in favor of the low frequency mode (CARMs have gain in the operating mode at two frequencies) and to enter into the CARM's efficient operating regime, it is necessary that the interaction cavity have a high Q for the higher frequency only. A frequency selective cavity can be achieved by using Bragg reflectors. In our CARM oscillator, we will use the Hamming-Window reflectors which were discussed in the previous section. The unit with the higher reflectivity will be placed on the upstream end of the interaction circuit and the lower reflectivity unit will determine the downstream end. The cavity Q has been measured to be 2000. Figure 9 is a schematic of the experiment under construction.

We also collaborated with Drs. Caplan and Kulke of LLNL on the development of a high frequency CARM oscillator driven by an induction linac. We provided the superconducting solenoid and were responsible for the rf measurements. The experiment resulted in the generation of megawatts at frequencies above 170 GHz.

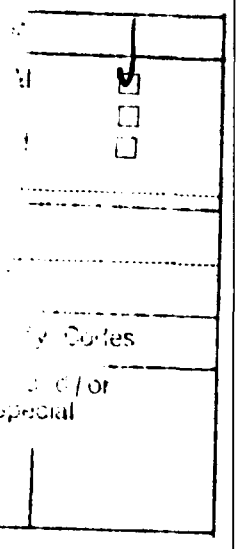

5. Tunable Gyro-BWO

We have constructed a tunable 100 kW, 60 GHz gyro-BWO experiment. This device could be used to drive extremely high power amplifiers, such as FELs and CARMs. Fast timescale tunability ($\simeq$ 3%) is achieved by changing the gun voltage, which affects the electron pitch angle, while broader slow timescale tunability ($\simeq$ 30%) is obtained by varying the magnetic field. To achieve continuous tunability, it is necessary to keep the beam from locking onto other modes in either gyrotron or other gyro-BWO interactions. We have designed the interaction tube to suppress all unwanted modes. To interrupt the azimuthal wall currents of the unwanted modes, the interaction tube has been slotted axially with three severs separated in azimuth by 120°. This destroys all modes without a third order azimuthal symmetry. The lowest order mode in the slotted tube is the desired TE_{31} mode. The TE_{61} and TE_{32} modes are the next lowest order modes and their cutoff frequencies are safely twice as high. Strong interaction will occur in the TE_{31} mode because it peaks at nearly the same radius as the TE_{01} mode, for which our 60 GHz MIG guns were designed. The experimental design parameters are listed in Table 4.

Nearly 100 kW is predicted from simulation in the frequency range of 46-63 GHz. The major items for the experiment were donated by industry. Hughes EDD gave us the superconducting solenoid from their 60 GHz gyrotron program and Varian gave us two MIG guns removed from two of their 60 GHz gyrotrons. The interaction circuit and the lossy drift superconducting solenoid's dewar has been built. The self-consistent gyro-BWO simulation code acquired from Dr. Caplan has been modified to account for linear polarization and then used to check the effect of a finite VSWR on the performance of a gyro-BWO and to predict the behavior of our design. The predicted tunability of our gyro-BWO described in Table 4 is shown in Fig. 10.

6. Gyro-Klystron Amplifier

In addition to the above, we have begun the design and construction of a high power, highly efficient 60 GHz fundamental gyro-klystron amplifier. Because of a more gradual and efficient bunching process, gyro-klystrons are predicted to be even more efficient than gyrotrons. The major items for this experiment have also been donated by industry. The superconducting solenoid is from the Hughes 94 GHz gyro-TWT program and the electron gun will be the second of the two 60 GHz gyrotron MIG guns from Varian. We have built a table to hold the superconducting solenoid's dewar. Our experiment will extend the initial Varian experimental study of the gyro-klystron carried out in 1978. We will also use cylindrical TE_{011} cavities with a length of 1.5 λ, but we will use three of them rather than just two. To avoid oscillation in the two drift tubes with a length of 5 cm, they will be slotted axially to interrupt the azimuthal wall currents. To help design the three cavity amplifier, we have obtained the self-consistent simulation code which Dr. K.R. Chu wrote for the University of Maryland's high power gyro-klystron amplifier project. Varian has offered to help benchmark the code by supplying us with the data from their gyro-klystron experiment.

MANUSCRIPTS AND PRESENTATIONS

"CARM Amplifier Designs for High Power," Q.S. Wang, D.B. McDermott and N.C. Luhmann, Jr., *J. of Infrared and Millimeter Waves*, 12, 297 (1991).

Prebunched High Harmonic Gyrotron," C.S. Kou, D.B. McDermott, N.C. Luhmann, Jr. and K.R. Chu, *IEEE Trans. Plasma Physics* 18, 343 (1990).

"Operation of a Large Orbit, High Harmonic Gyro-Traveling Wave Tube Amplifier," D.S. Furuno, D.B. McDermott, C.S. Kou, N.C. Luhmann, Jr. and P. Vitello, *IEEE Trans. Plasma Physics* 18, 313 (1990).

"Theoretical and Experimental Investigation of a High-Harmonic Gyro-Traveling-Wave-Tube Amplifier," D.S. Furuno, D.B. McDermott, C.S. Kou, N.C. Luhmann, Jr., and P. Vitello, *Phys. Rev. Lett.* 62, 1314 (1988).

"A Four Cavity, High Harmonic Gyroklystron Amplifier," D.S. Furuno, D.B. McDermott, H. Cao, C.S. Kou, N.C. Luhmann, Jr., P. Vitello and K. Ko, *Int. J. Electronics*, 65, 429 (1988).

"Operation of a Large Orbit, High Harmonic Multicavity Gyro-Klystron Amplifier," D.S. Furuno, D.B. McDermott, N.C. Luhmann, Jr., P. Vitello and K. Ko, *IEEE Trans. Plasma Science*, 16, 155 (1988).

"Bragg Reflectors: Sinusoidal versus Rectangular," C.K. Chong, D.B. McDermott, M.M. Razeghi and N.C. Luhmann, Jr., *1990 Conf. of APS Div. of Plasma Physics.*

"Optimization of Magnetic Field Taper for CARM," Q.S. Wang, G. Vasilakos, D.B. McDermott and N.C. Luhmann, Jr. *1990 Conf. of APS Div. of Plasma Physics.*

"Design and Optimization of a 100 kW Gyro-TWT," C.S. Kou, D.B. McDermott, C.K. Chong and N.C. Luhmann, Jr., *Conf. of APS Plasma Physics Division.*

"100 kW, 54-70 GHz Gyro-BWO," T.R. Stephenson, G. Vasilakos, G.D. Ramlow, D.B. McDermott, N.C. Luhmann, Jr. and M. Caplan, *Conf. of APS Division of Plasma Physics.*

"Bragg Reflectors: Sinusoidal Versus Rectangular Corrugation," C.K. Chong, D.B. McDermott, M.M. Razeghi, N.C. Luhmann, Jr., M. Thumm and J. Pretterebner, *Digest of 1990 Int. Conf. on IR and mm-Waves.*

"Nonlinear Self-Consistent Analysis for a Two-Stage Gyro-TWT Amplifier," C.S. Kou, D.B. McDermott and N.C. Luhmann, Jr., *Digest of 1990 Int. Conf. on IR and mm-Waves.*

"CARM Design for Heating High Field Tokamak," Q.S. Wang, D.B., McDermott and N.C. Luhmann, Jr., *Digest of 1990 Int. Conf. on IR and mm-Waves.*

"Bragg Reflectors: Tapered and Untapered," C.K. Chong, M.M. Razeghi, D.B. McDermott, N.C. Luhmann, Jr., M. Thumm and J. Pretterebner, *1991 SPIE Conf. on Beams and High Power Microwaves.*

"Magnetically Tapered CARM for High Power," Q.S. Wang, D.B. McDermott and N.C. Luhmann, Jr., *1991 SPIE Conf. on Beams and High Power Microwaves.*

"Bragg Resonator for Selective Feedback in Overmoded Oscillators," C.K. Chong, D.B. McDermott, M.M. Razeghi, N.C. Luhmann, Jr., M. Caplan and B. Kulke, *Digest of 1990 SPIE Conf. on Intense Microwave and Particle Beams* 1226, 228 (1990).

"High Power CARM for High Gradient RF Linac," Q.S. Wang, D.B. McDermott, A.T. Lin, N.C. Luhmann, Jr. and K.R. Chu, *Digest of 1990 SPIE Conf. on Intense Microwave and Particle Beams* 1226, 220 (1990).

"Bragg Resonator for Selective Feedback in Overmoded Oscillators," C.K. Chong, M.M. Razeghi, D.B. McDermott and N.C. Luhmann, Jr., *Proceedings of 1990 IEEE Int. Conf. on Plasma Science.*

"High Power CARM for High Gradient RF Linac," Q.S. Wang, D.B. McDermott, A.T. Lin, N.C. Luhmann, Jr. and K.R. Chu, *Proceedings of 1990 IEEE Int. Conf. on Plasma Science.*

"Prebunched High Harmonic Gyrotron-Magnicon," C.S. Kou, D.B. McDermott and N.C. Luhmann, Jr., *Proceedings of 1990 IEEE Conf. on Plasma Science.*

"High Power CARM Amplifier," Q.S. Wang, A.T. Lin, N.C. Luhmann, Jr. and D.B. McDermott, *1990 Microwave Power Tube Conf.*

"Design of a Bragg Resonator," C.K. Chong, D.B. McDermott, M. Razeghi and N.C. Luhmann, Jr., *Bull. Am. Phys. Society* 34, 2089 (1989).

"Design of a 100 kW Gyro-TWT," C.S. Kou, D.B. McDermott, C.K. Chong and N.C. Luhmann, Jr., *Bull. Am. Phys. Society* 34, 2092 (1989).

"Bragg Resonator for Selective Feedback in Overmoded Oscillators," C.K. Chong, D.B. McDermott, M. Razeghi and N.C. Luhmann, Jr., *Digest of 1989 Int. Conf. on Infrared and Millimeter Waves*, Wurzburg, Germany.

"Design of a 100 kW Gyro-TWT," C.S. Kou, D.B. McDermott, C.K. Chong and N.C. Luhmann, Jr., *Digest of 1989 Int. Conf. on Infrared and Millimeter Waves*, Wurzburg, Germany.

"Cyclotron Autoresonance Maser Amplifier and Oscillators," C.K. Chong, M.M. Razeghi, D.B. McDermott, N.C. Luhmann, Jr., M. Caplan and B. Kulke, *Digest of 1989 IEDM Conference,* Washington, D.C.

"Design of a 100 kW Gyro-TWT," C.S. Kou, D.B. McDermott, C.K. Chong and N.C. Luhmann, Jr., *Proc. of SPIE's Symp. on Microwave and Particle Beam Sources and Directed Energy Concepts*, ISBN 0 – 8194 – 0096 – 3, p. 269, Los Angeles, California (1989).

"Design of a 1 MW Gyro-TWT," D.B. McDermott, C.S. Kou and N.C. Luhmann, Jr., *Bull. of APS*, 33, 2085 (1988).

"High Harmonic Gyro-Amplifiers," D.S. Furuno, D.B. McDermott, N.C. Luhmann, Jr., and P. Vitello, *Proceedings of Second Asia-Pacific Microwave Conf.*, Beijing, China (1988).

"Design of a 100 kW Gyro-TWT," C.S. Kou, D.B. McDermott, C.K. Chong and N.C. Luhmann, Jr., *Digest of 13th Int. Conf. IR & mm-Waves*, Honolulu, Hawaii (1988).

"High Harmonic Gyro-Amplifiers," D.S. Furuno, D.B. McDermott and N.C. Luhmann, Jr., *Digest of 1988 Microwave Power Tube Conference*, Monterey, California.

"Theory, Design and Operation of a High Harmonic Multicavity Gyro-Klystron Amplifier," D.B. McDermott, D.S. Furuno, N.C. Luhmann, Jr., P. Vitello and K. Ko, *Bull. of Amer. Phy. Soc.* 32, 1864 (1987).

"Operation of a High Harmonic Gyo-TWT Amplifier," D.S. Furuno, D.B. McDermott, N.C. Luhmann, Jr. and P. Vitello, *Bull. of Amer. Phy. Soc.* 32, 1864 (1987).

"Results of a Large Orbit, High Harmonic Gyro-TWT Amplifier," D.S. Furuno, D.B. McDermott and N.C. Luhmann, Jr., *Conf. Digest Twelfth Int. Conf. Infrared and Millimeter Waves* IEEE #87CH2490-1, 330 (1987).

"Operation of a Large Orbit, High Harmonic Gyro-TWT Amplifier," D.S. Furuno, D.B.McDermott and N.C. Luhmann, Jr., *Tech. Digest Int. Electron Devices Meeting* IEEE #87CH2515-5, 817 (1987).

Table 1. Optimized parameters of the fundamental harmonic 35 GHz gyro-TWT (Case a) and second harmonic 35 GHz gyro-TWT (Case b).

	Case a	Case b
Waveguide radius (r_w)	0.26 cm	0.44 cm
Operating mode	TE_{11}	TE_{21}
Operating cyclotron harmonic (s)	1	2
Beam voltage (V_b)	100 kV	100 kV
Beam current (I_b)	5 A	25 A
Guiding center position (r_c)	0.35 r_w	0
Electron velocity ratio α ($= v_\perp/v_z$)	1.0	1.0
Axial velocity spread ($\Delta v_z/v_z$)	5%	5%
Magnetic field B	12.4 kG	6.2 kG
B/B_g^*	0.98	0.98
Power	130 kW	830 kW
Efficiency	26.4%	33%
Bandwidth	13%	11.4%

*B_g is the magnetic field which results in grazing intersection between the operating mode and the operating harmonic line.

Table 2. Parameters of Hamming-Window Bragg Reflectors Fabricated for 10.6 GHz Gyro-TWT/CARM Oscillator Experiment: (a) gun-side and (b) output end.

	Case a	Case b
period	1.500 cm	1.500 cm
minimum radius	1.809 cm	1.809 cm
corrugation amplitude	0.400 cm	0.325 cm
corrugation length	31.50 cm	31.50 cm
ω/ω_c	2.2	2.2
corrugation orientation	positive	positive
corrugation profile	tapered	tapered
corrugation geometry	rectangular	rectangular

Table 3. High Peak Power CARM Amplifier Design

Voltage	**1.5**	**MV**
Beam Current	**300**	**A**
Output Power	**155**	**MW**
Frequency	**17**	**GHz**
Efficiency	**34.3%**	
$\alpha(=v_\perp/v_\parallel)$	0.5	
$\Delta v_\parallel/v_\parallel$	0.7%	
Waveguide Mode	TE_{11}	
Circuit Radius	2.08	cm
Beam Radius (in circuit)	0.56	cm
Magnetic Field (CARM)	3.87	kG
Magnetic Field Taper	-1.2%	cm^{-1}
B/B_g	1.3	
ω/ω_c	4.0	
Linear Gain	0.5	dB/cm
Duty Cycle	0.1%	
Wall Loading	0.6	W/cm^2

Table 4. Parameters of Proposed Gyro-BWO

Frequency	46-63 GHz
Power	100 kW
Efficiency	10%
Voltage	70-80 kV
Beam Current	5-11 A
$\alpha(=v_\perp/v_\parallel)$	1.5
Magnetic Field	20-30 kG
Mode	TE_{31}
Cavity Radius	0.454 cm
Cavity Length	6 cm

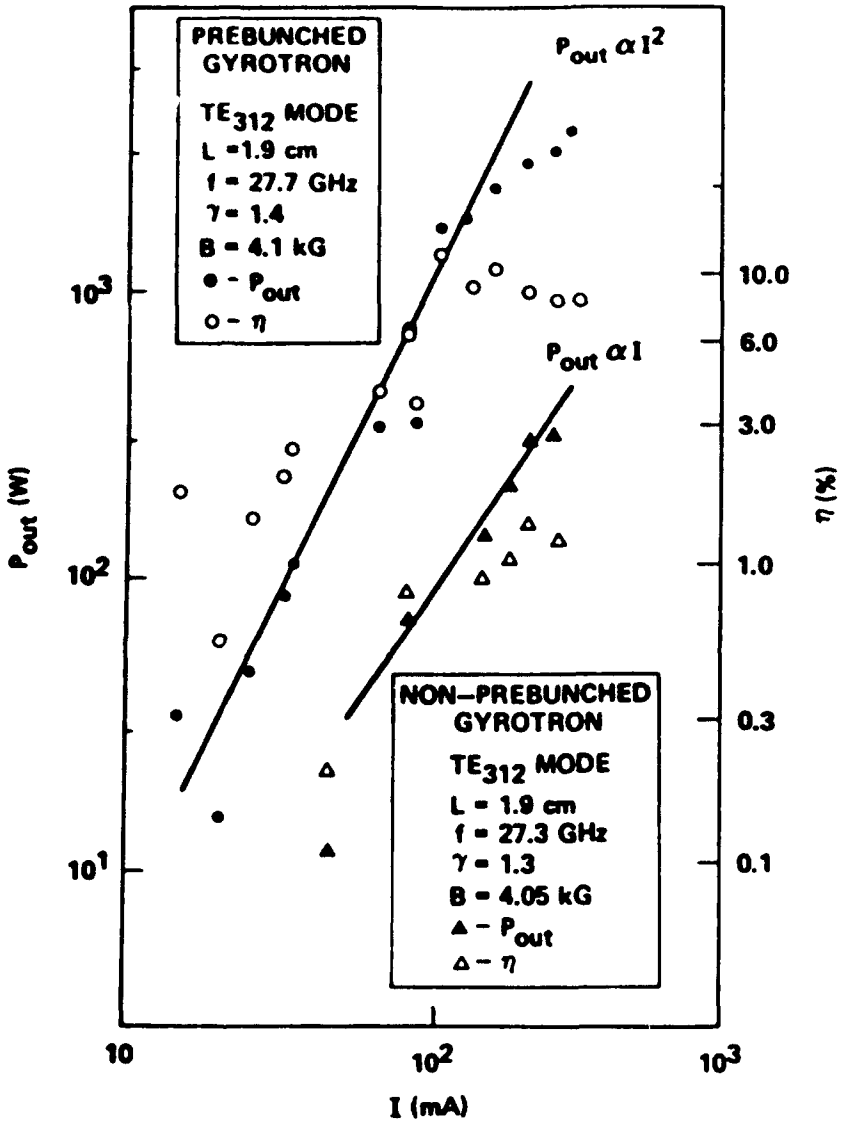

Figure 1. Dependence of measured output power on current of the prebunched harmonic gyrotron and an equivalent nonprebunched harmonic gyrotron.

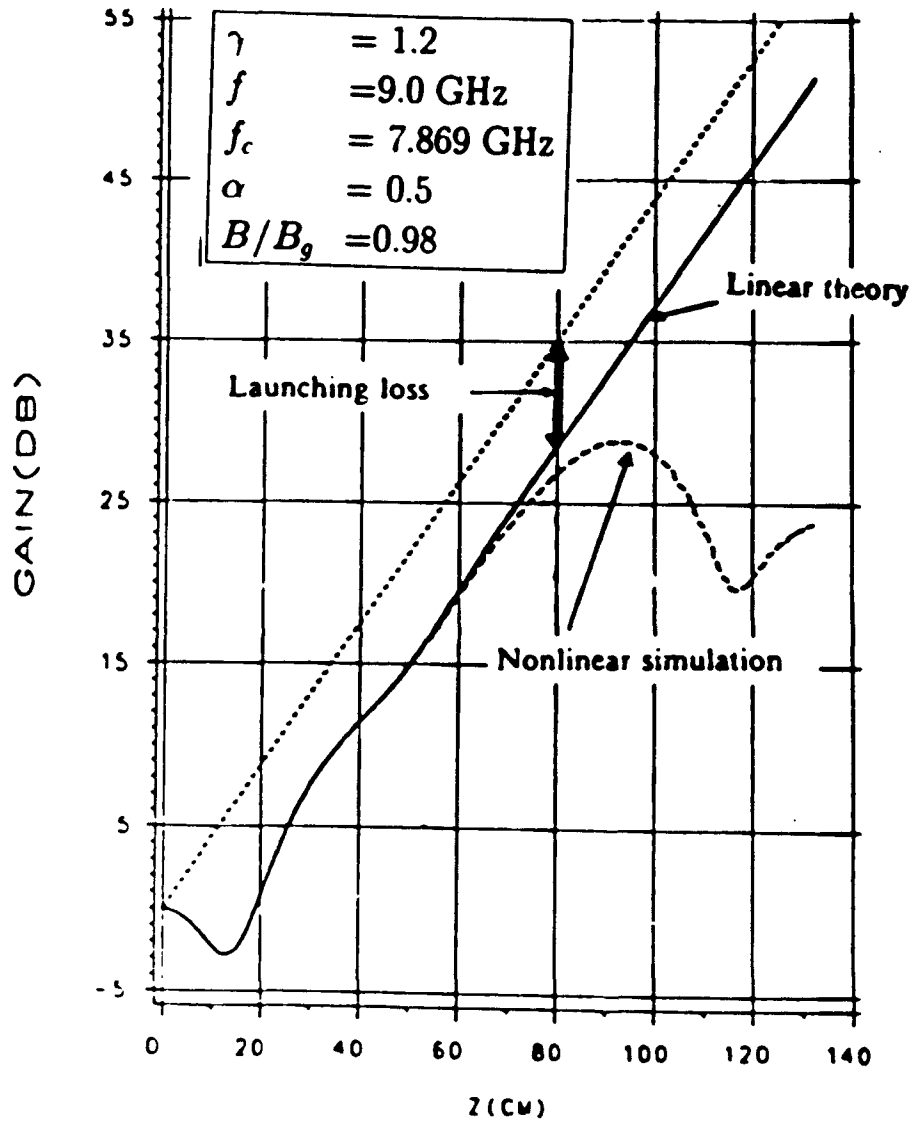

Figure 2. Spatial growth of output power in fundamental TE_{11} gyro-TWT for our device from simulation (solid curve) and from analytical theory (wide dashed curve). The narrow dashed curve is a line through the origin and parallel to the linear gain line.

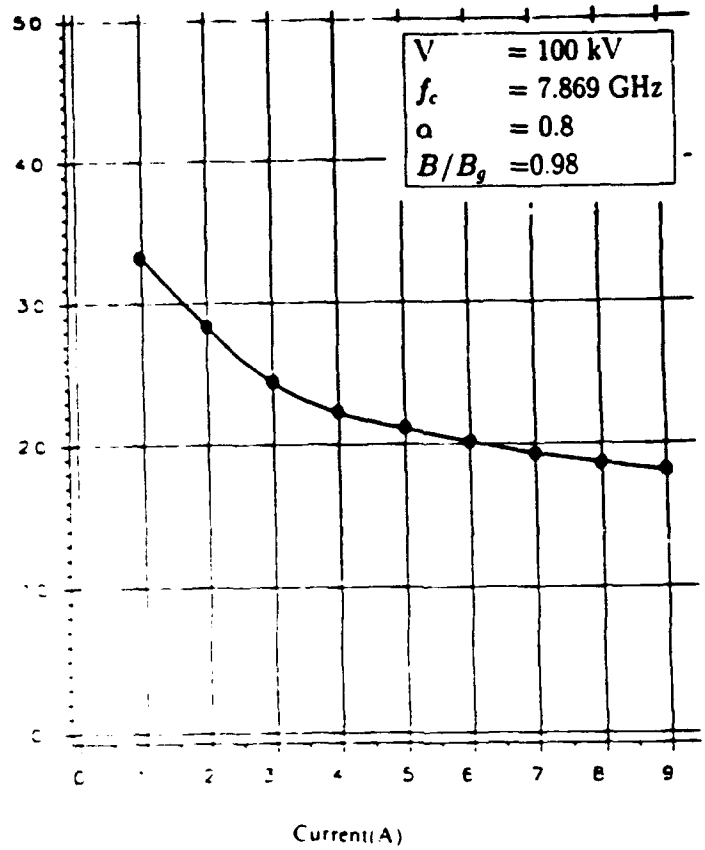

Figure 3. Dependence of start oscillation length on electron beam current for the second harmonic gyro-BWO interaction in the TE_{21} mode.

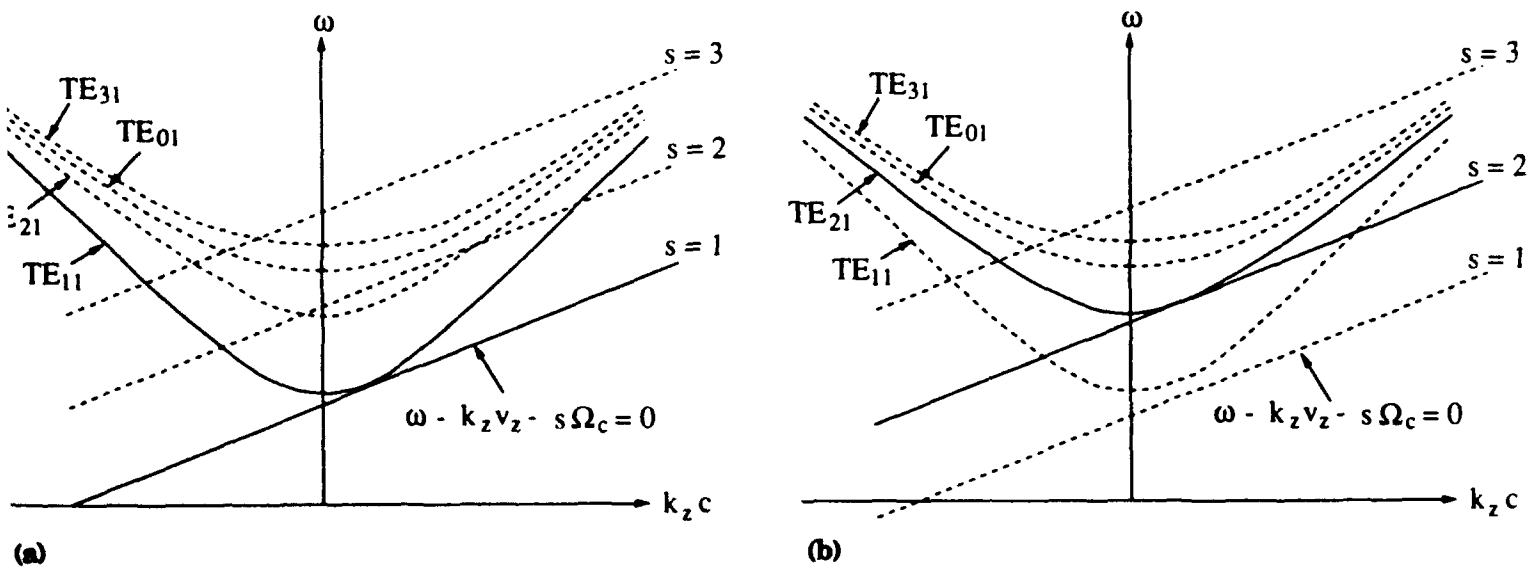

Figure 4. Uncoupled dispersion diagram of operating mode (intersection of unbroken curves) and likely oscillating modes (intersections with $k_z < 0$) for a) fundamental TE_{11} mode gyro-TWT and b) second harmonic TE_{21} mode gyro-TWT.

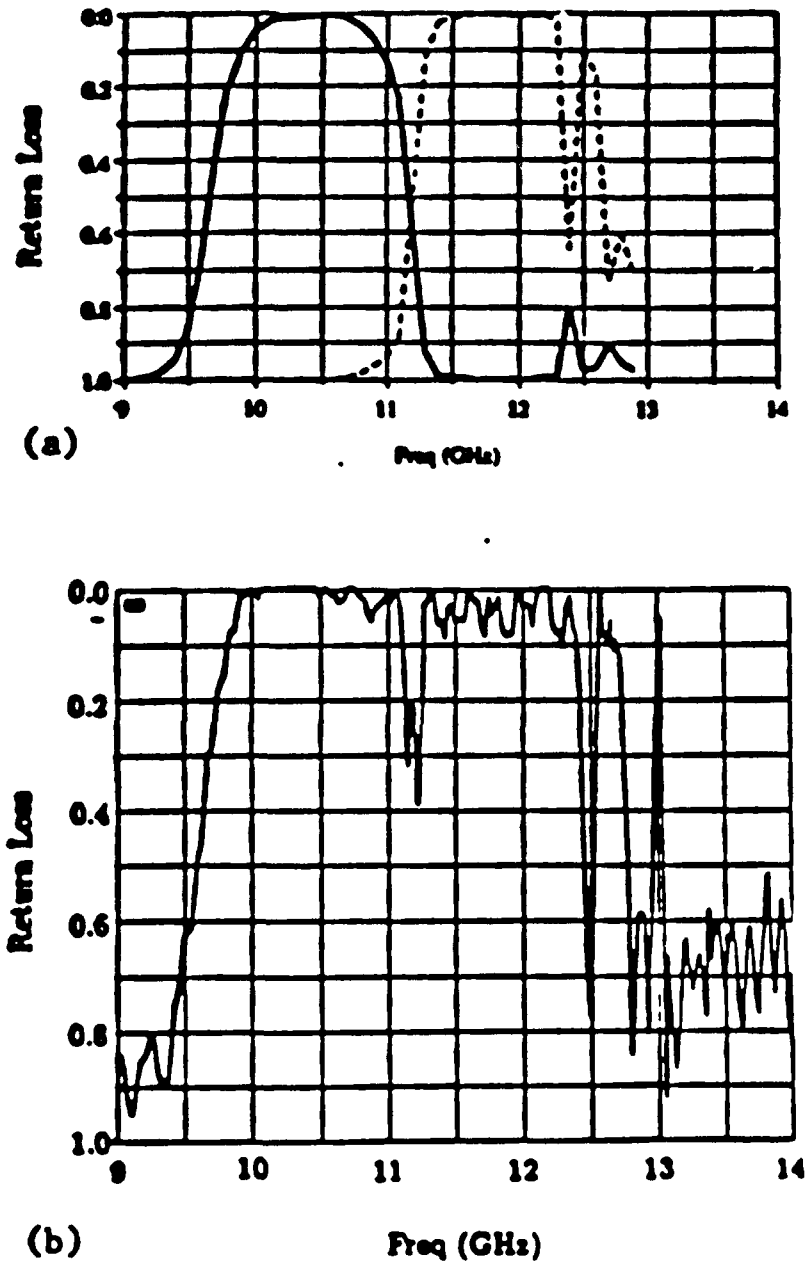

Figure 5. Frequency dependence of reflection in the TE_{11} and TM_{11} modes from a single Hamming-Window reflector described in Table 2(a) from a) scattering matrix simulation and b) measurement.

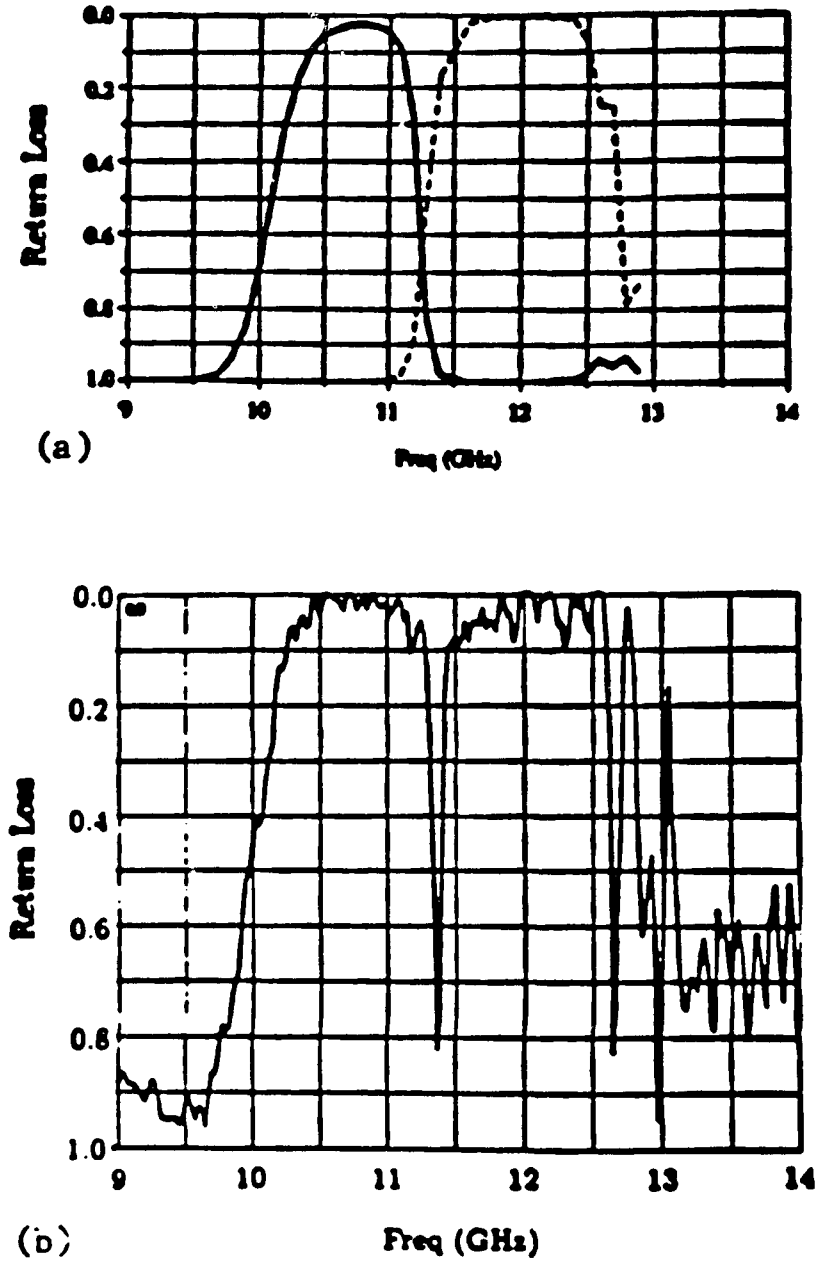

Figure 6. Frequency dependence of reflection in the TE_{11} and TM_{11} modes from a single Hamming-Window reflector described in Table 2(b) from a) scattering matrix simulation and b) measurement.

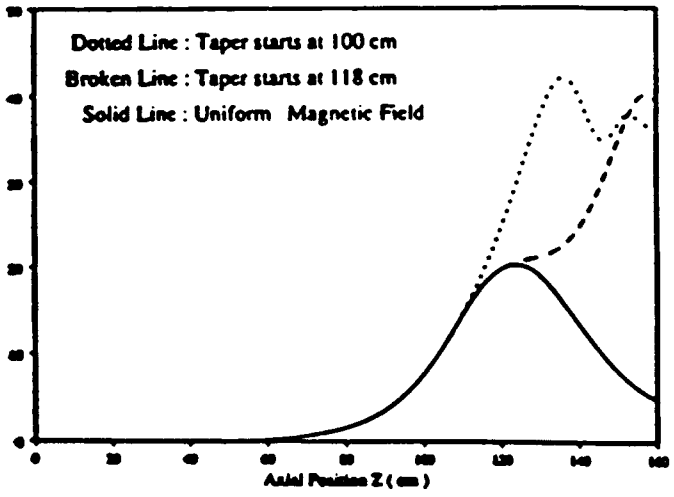

Figure 7. Efficiency as function of axial position for CARM in Table 2 for three cases of magnetic taper.

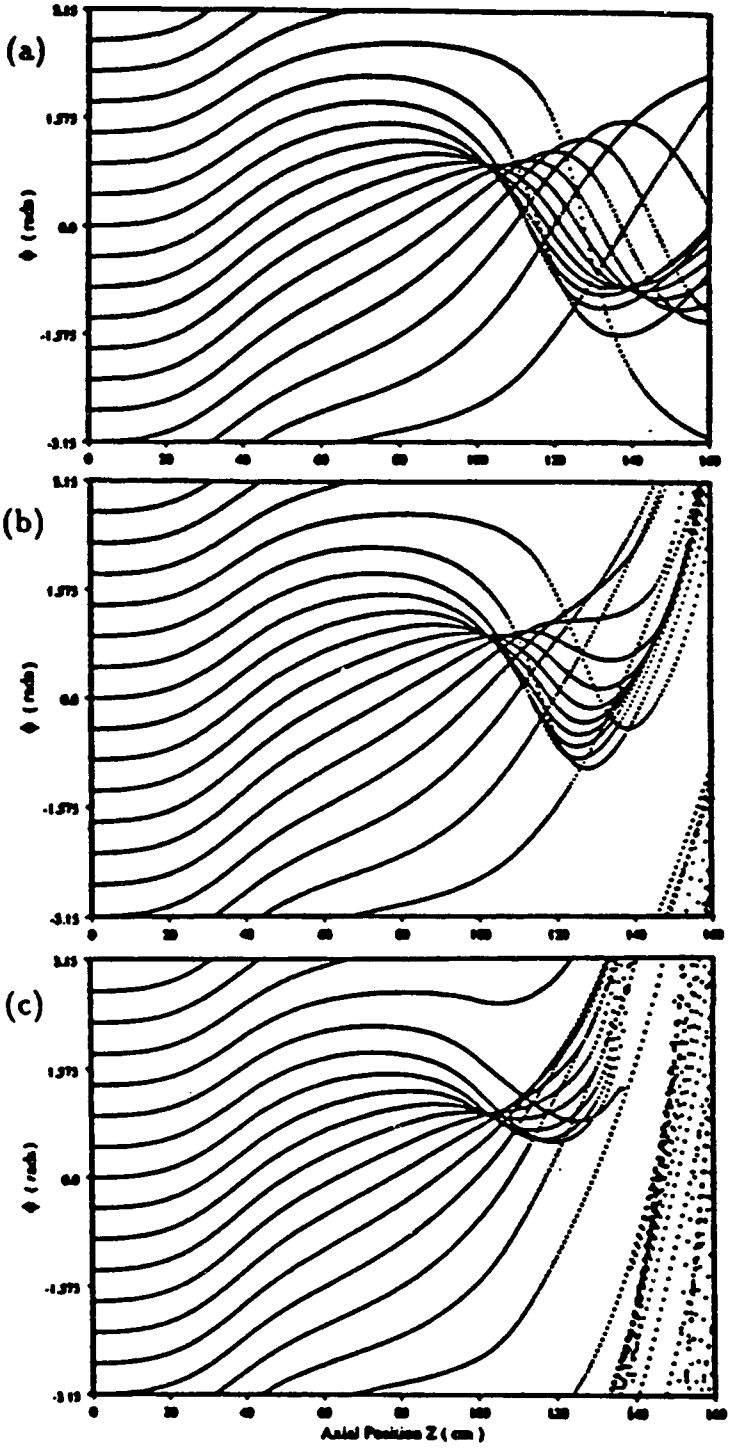

Figure 8. Electron phase evolution along the tube length of 1.5 MV, 300 A CARM amplifier described with Table 2 with a) uniform magnetic field, b) magnetic taper of - 1.4%/cm beginning at z = 118 cm and c) magnetic taper of -1.4%/cm beginning at z = 100 cm (17 GHz, TE_{11} , $\omega/\omega_c = 4$, B/B_g = 1.3, $\alpha = 0.5$, $\Delta v_{\|}/v_{\|} = 0$).

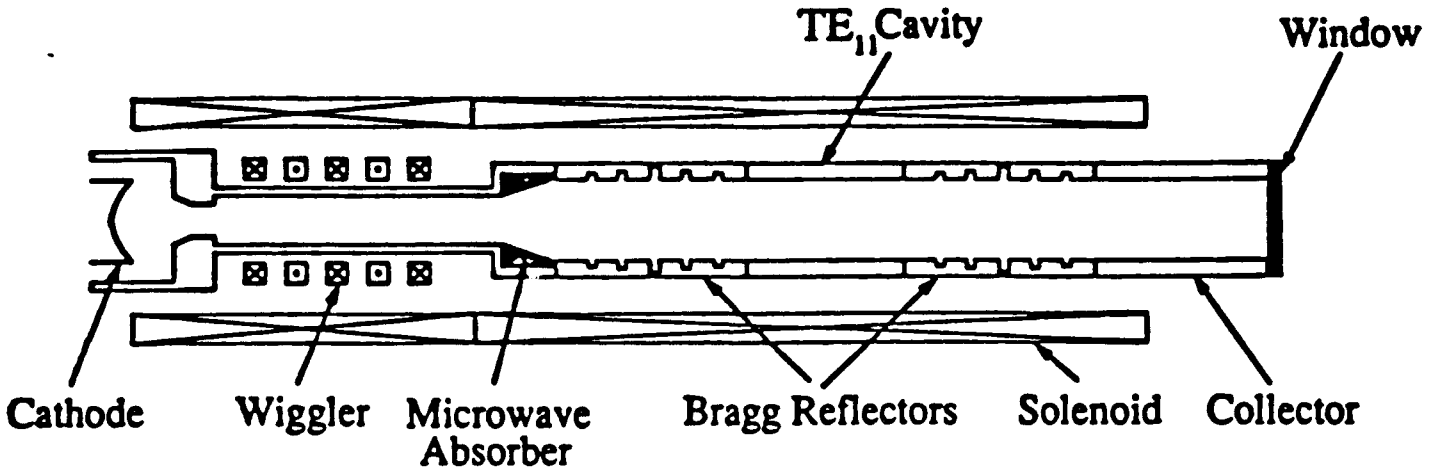

Figure 9. Schematic of our 400 kV, 10.6 GHz CARM oscillator experiment with a high Q Hamming-Window Bragg reflector.

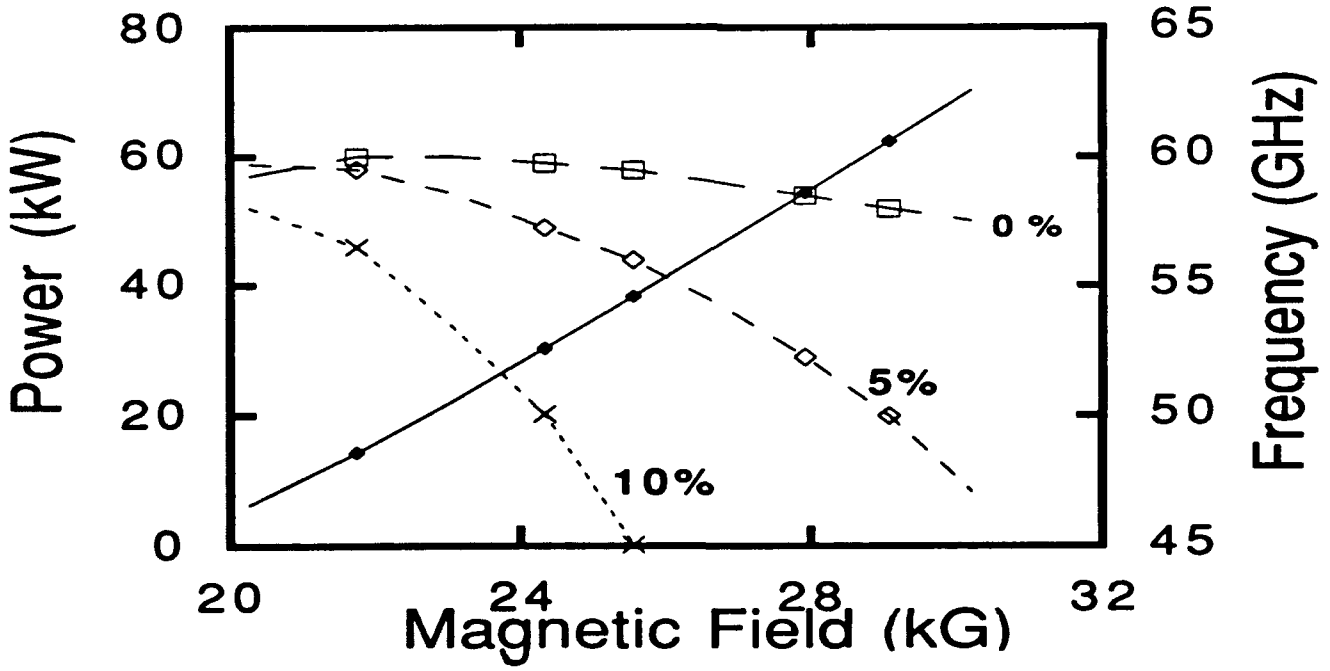

Figure 10. For several values of axial velocity spread, the dependence of output frequency (solid diamond) and power (empty squares for $\Delta v_{\|}/v_{\|}$ = 0%, empty diamonds for $\Delta v_{\|}/v_{\|}$ = 5% and crosses for $\Delta v_{\|}/v_{\|}$ = 10%) on axial magnetic field.